AMERICAN SOCIETY FOR MICROBIOLOGY | Journal of Virology®

PATHOGENESIS AND IMMUNITY

Canine Distemper Virus Spread and Transmission to Naive Ferrets: Selective Pressure on Signaling Lymphocyte Activation Molecule-Dependent Entry

Bevan Sawatsky,[a,b] Roberto Cattaneo,[c] Veronika von Messling[a,b]

[a]Division of Veterinary Medicine, Paul-Ehrlich-Institut, Federal Institute for Vaccines and Biomedicines, Langen, Germany

[b]German Center for Infection Research, TTU Emerging Infections, Langen, Germany

[c]Department of Molecular Medicine, Virology and Gene Therapy Track, Mayo Clinic College of Medicine, Rochester, Minnesota, USA

ABSTRACT Upon infection, morbilliviruses such as measles virus, rinderpest virus, and canine distemper virus (CDV) initially target immune cells via the signaling lymphocyte activation molecule (SLAM) before spreading to respiratory epithelia through the adherens junction protein nectin-4. However, the roles of these receptors in transmission from infected to naive hosts have not yet been formally tested. To experimentally addressing this question, we established a model of CDV contact transmission between ferrets. We show here that transmission of wild-type CDV sometimes precedes the onset of clinical disease. In contrast, transmission was not observed in most animals infected with SLAM- or nectin-4-blind CDVs, even though all animals infected with the nectin-4-blind virus developed sustained viremia. There was an unexpected case of transmission of a nectin-4-blind virus, possibly due to biting. Another unprecedented event was transient viremia in an infection with a SLAM-blind virus. We identified three compensatory mutations within or near the SLAM-binding surface of the attachment protein. A recombinant CDV expressing the mutated attachment protein regained the ability to infect ferret lymphocytes *in vitro*, but its replication was not as efficient as that of wild-type CDV. Ferrets infected with this virus developed transient viremia and fever, but there was no transmission to naive contacts. Our study supports the importance of epithelial cell infection and of sequential CDV H protein interactions first with SLAM and then nectin-4 receptors for transmission to naive hosts. It also highlights the *in vivo* selection pressure on the H protein interactions with SLAM.

IMPORTANCE Morbilliviruses such as measles virus, rinderpest virus, and canine distemper virus (CDV) are highly contagious. Despite extensive knowledge of how morbilliviruses interact with their receptors, little is known about how those interactions influence viral transmission to naive hosts. In a ferret model of CDV contact transmission, we showed that sequential use of the signaling lymphocytic activation molecule (SLAM) and nectin-4 receptors is essential for transmission. In one animal infected with a SLAM-blind CDV, we documented mild viremia due to the acquisition of three compensatory mutations within or near the SLAM-binding surface. The interaction, however, was not sufficient to cause disease or sustain transmission to naive contacts. This work confirms the sequential roles of SLAM and nectin-4 in morbillivirus transmission and highlights the selective pressure directed toward productive interactions with SLAM.

KEYWORDS canine distemper virus, CDV, compensatory mutations, contact transmission, morbilliviruses, nectin-4, selective pressure, signaling lymphocyte activation molecule, SLAM

Received 18 April 2018 **Accepted** 14 May 2018

Accepted manuscript posted online 23 May 2018

Citation Sawatsky B, Cattaneo R, von Messling V. 2018. Canine distemper virus spread and transmission to naive ferrets: selective pressure on signaling lymphocyte activation molecule-dependent entry. J Virol 92:e00669-18. https://doi.org/10.1128/JVI.00669-18.

Editor Terence S. Dermody, University of Pittsburgh School of Medicine

Address correspondence to Bevan Sawatsky, bevan.sawatsky@pei.de.

The *Morbillivirus* genus comprises viruses with a diverse vertebrate host range, including measles virus (MeV), which infects humans and nonhuman primates, rinderpest and peste-des-petits-ruminants viruses, which target large and small ruminants, and canine distemper virus (CDV), which infects a broad range of terrestrial carnivores, including dogs and ferrets (1). With an estimated basic reproduction number (R_0) of 12 to 18 for MeV (2), morbilliviruses are among the most contagious infectious agents known. Effective vaccines are available for the aforementioned viruses, although high vaccination rates are required to prevent outbreaks in susceptible populations. Rinderpest was recently declared eradicated in cattle, which is due in large part to a successful worldwide vaccination campaign, and similar progress could be made for measles by increasing vaccine coverage (3).

MeV is markedly more contagious than other respiratory pathogens such as pandemic influenza viruses (4, 5). This high transmissibility of morbilliviruses is thought to be largely due to extensive replication and release of infectious virus in the respiratory tract during later infection stages, when infected individuals or animals show signs of clinical disease (6, 7). Damage and irritation in the upper respiratory tract during this phase can trigger sneezing and coughing, which in turn generate droplets and aerosols that can spread widely. MeV can be stable in indoor environments for several days, and there is a high risk for viral transmission by contaminated fomites in health care environments such as hospitals (8). While MeV and influenza virus are often associated with airborne transmission, direct contact transmission also plays a significant role. The airborne transmission route imposes a high selective barrier to transmission where the diversity of the transmitted virus population is low (7, 9), whereas contact transmission presents a lower barrier allowing larger doses of more diverse viral loads to be transferred (9, 10). The mode of contact transmission is therefore an important consideration in outbreak investigations (8, 11).

Two cellular receptors have been identified for morbilliviruses: signaling lymphocyte activation molecule (SLAM or CD150) and nectin-4. SLAM is expressed on B and T cells, as well as certain subsets of dendritic cells (DCs) and macrophages (12–14), and it serves as the primary immune cell receptor. At initial infection stages, virus entering the upper respiratory tract comes into contact with SLAM-positive immune cells, most likely tissue-resident DCs or alveolar macrophages. These cells then traffic to local draining lymph nodes, where the virus spreads to T and B cells. Within 1 week after infection, virtually the entire lymphatic system is colonized (15–17). Infected circulating immune cells subsequently spread the virus to epithelial cells via contact with nectin-4, which is expressed on the basolateral side of the apical junction complexes (18, 19). Virus then invades the epithelium and, after replication in epithelial cells, is released into the upper respiratory tract, where it can be transmitted to the next host (20–24).

Morbilliviruses must be shed into the airways for efficient infection of the next host. Monkeys infected with a recombinant MeV that does not bind nectin-4 and ferrets infected with an analogous nectin-4-blind CDV do not shed detectable virus in bronchoalveolar lavage fluids or urine (25, 26). This implies that epithelial cell infection is important for transmission. In contrast, SLAM binding is required to establish systemic morbillivirus infection. However, monkeys and ferrets infected with either SLAM-blind MeV or CDV, respectively, produce strong immune responses against these viruses despite a lack of viremia (27, 28). The fact that SLAM-blind viruses infect and efficiently replicate in epithelial cells may provide an explanation for this apparent discrepancy, but it also implies that local replication in the respiratory epithelium could result in low-efficiency transmission.

To address the respective roles of SLAM and nectin-4 in virus transmission to naive contact animals, we infected ferrets with wild-type CDV or with viruses blind to either receptor. Transmission was monitored over prolonged periods of contact, as well as during shorter defined periods spanning the onset of clinical signs of disease. We show formally that receptor-blind viruses are not readily transmissible, even in the more permissive contact transmission model. We also document that contact transmission precedes clinical signs by approximately 1 day. Finally, our analysis of the biological

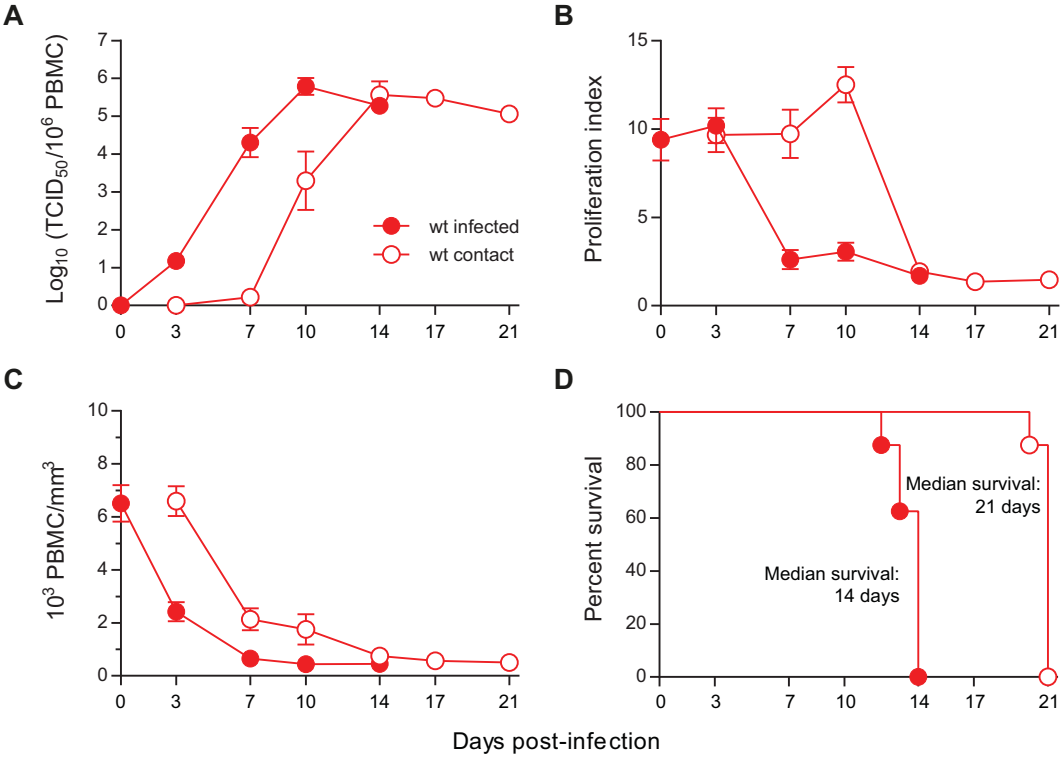

FIG 1 Efficient transmission of wild-type CDV to naive contact animals. Eight ferrets were infected intranasally with 2×10^5 $TCID_{50}$ of the wild-type (wt) strain 5804PeH and were then each cohoused with one naive contact animal after 3 days (n = 8 infected/contact pairs). (A) The course of cell-associated viremia is shown as the $\log_{10}$ of the virus titer per 10^6 PBMCs. (B) *In vitro* proliferation activity of lymphocytes from infected and contact animals. (C) Total PBMC counts from infected and contact animals, shown as 10^3 leukocytes per mm^3. (D) Survival of infected and contact animals. The death of an animal is indicated by a step down on the curve, and median survival for each group is indicated on the graphs. Days postinfection are indicated on the *x* axes of the graphs, and error bars represent standard error of the mean.

characteristics of a pseudorevertant SLAM-blind virus illustrates the strong selective pressure for efficient interaction of morbilliviruses with SLAM.

RESULTS

Wild-type CDV contact transmission is highly efficient. Even though morbilliviruses are airborne pathogens, close contact plays an important role in their epidemiology (11, 29). Host-to-host transmission assesses the ability of virus to be shed by an infected animal and subsequently establish a successful infection in a naive contact. Contact transmission results in more frequent exposure to higher viral doses than the airborne route (9, 10), increasing the likelihood that transmission events will be observed, although aerosols still contribute to transmission in this context. It is also distinct from direct infection, which evaluates infectivity under ideal circumstances. To determine the efficiency of CDV transmission during a prolonged contact period, ferrets were infected with the wild-type CDV strain 5804PeH (30, 31) and then cohoused with uninfected contact animals, starting 3 days after infection. Viremia was first detected on day 3 after infection and peaked between days 7 and 10 (Fig. 1A), reflecting the typical range for this virus (32), with corresponding decreases in lymphocyte proliferation (Fig. 1B) and total white blood cell counts (Fig. 1C). The infected animals were sacrificed between days 12 and 13 after infection, when they reached experimental endpoints (Fig. 1D).

In contact animals, robust viremia was detected 7 days after cohousing with infected animals (Fig. 1A). As in previous studies (33), onset of leukopenia was already observed at the 3-day time point, when virus was detectable at only very low levels (Fig. 1C), while lymphocyte proliferation inhibition followed kinetics similar to those in the

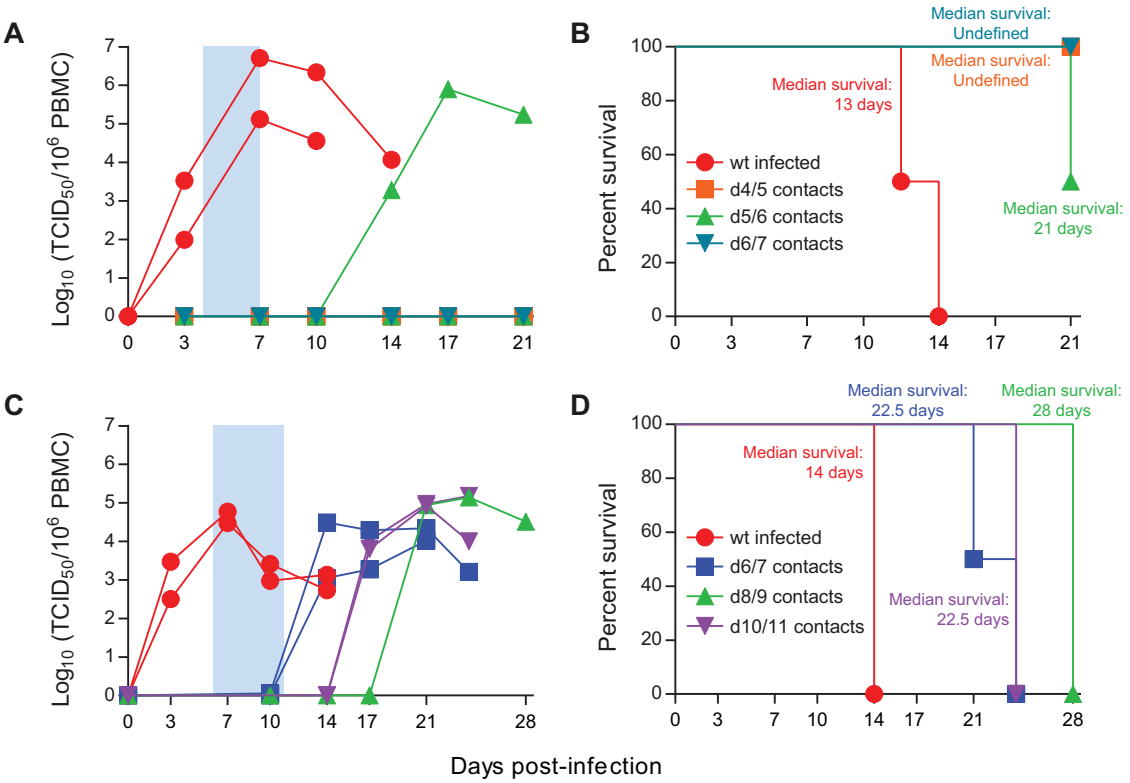

FIG 2 Kinetics of wild-type CDV transmission to naive contact animals. Ferrets were infected intranasally with 2×10^5 $TCID_{50}$ of the wild-type strain 5804PeH and then cohoused for consecutive 24-h periods immediately preceding the onset of clinical signs (A and B) or for consecutive 48-h periods during and after the onset of clinical signs (C and D). (A and C) The course of cell-associated viremia is shown as the $\log_{10}$ of the virus titer per 10^6 PBMCs for contact exposure periods of 24 h between days 4 and 7 (A) and for 48 h between days 6 and 11 (C). (B and D) Survival of infected and contact animals for contact exposure periods of 24 h between days 4 and 7 (B) and for 48 h between days 6 and 11 (D). The death of an animal is indicated by a step down on the curve, and the color-coded median survival for each group is indicated on the graphs. Each series in panels A and C represents one animal ($n = 2$ infected with 2 contacts per contact window). Symbols for panels A and B are indicated in panel B, and those for panels C and D are indicated in panel D. Days postinfection are indicated on the *x* axes of the graphs.

originally infected animals, with a small peak on day 3 and the drop on day 7 after contact (Fig. 1B). Consistently, there was a 1-week delay in survival for the contact animals (Fig. 1D). These experiments demonstrate that wild-type CDV is efficiently transmitted in a setting involving prolonged contact and suggest that transmission occurs almost immediately after cohousing of the animals.

Efficient CDV transmission coincides with the onset of clinical signs. It is postulated that transmission starts when the first clinical signs are observed or slightly before (34–36). Detailed information about the earliest times of transmission is important for the effective public health management and epidemiological tracing of outbreaks. To assess the extent of transmission prior to the onset of clinical signs, we cohoused naive and infected animals for 24-h periods between days 4 and 7 after the initial infection with 5804PeH, which typically results in first signs of fever and rash at 7 to 8 days after infection (30). Out of all conditions tested, only one contact animal cohoused on days 5 to 6 became infected (Fig. 2A); it developed cell-associated viremia at around day 14 and succumbed to the disease approximately 1 week thereafter (Fig. 2B). Thus, transmission prior to the onset of clinical signs can occur occasionally and likely reflects individual differences in the course of dissemination.

We next investigated the effect of contact exposure at later times after initial infection. Naive and infected animals were cohoused for 48 h between days 6 and 11, spanning the period from slightly before the first appearance of fever and rash to severe systemic disease. Contact animals all developed clinical signs approximately 1 week after first exposure to the infected animal (Fig. 2C) and had a corresponding delay

in time to death (Fig. 2D), confirming the link between onset of clinical disease and transmission.

SLAM and nectin-4 receptors are required for transmission. The two phases of CDV infection and disease, colonization of immune tissues and spread to epithelia, are determined by interaction with the two receptors SLAM and nectin-4, respectively (37, 38). Evolutionary forces drive H protein variability during virus circulation, and compensatory mutations often arise at other positions that offset detrimental changes in the protein (39). By infecting susceptible animals with viruses that are no longer able to interact with either SLAM or nectin-4 (26, 27), we can gain insight into the compensatory mechanisms that affect the interactions between CDV and its receptors. We assessed the impact of receptor interactions on CDV transmission by cohousing naive and infected animals starting 3 days after initial infection. Only one of the animals infected with the SLAM-blind virus developed low-titer transient viremia on day 7 after infection (Fig. 3A), but transmission occurred in none of the pairs (Table 1). In contrast, cell-associated viremia was seen in all animals infected with the nectin-4-blind virus and lasted for 2 weeks (Fig. 3B). However, transmission occurred in only one pair between days 17 and 21 after initial infection, which represents a considerable delay compared to the 7- to 10-day period seen for the wild-type virus (Fig. 1). Neither the initially infected nor the contact animal displayed any clinical signs, suggesting that the virus had not mutated into a pathogenic phenotype.

While the lack of viremia in the contact animals is a strong indication that there was no transmission, we could not exclude that exposure to small amounts of virus resulted in subclinical infection (40). We thus assessed whether neutralizing antibodies against CDV were generated in selected infected/contact animal pairs prior to and after the transmission experiments. All animals were seronegative prior to infection, and only the infected animals developed detectable neutralizing responses after infection (Fig. 3C and D). Subsequent challenge with the wild-type 5804PeH strain revealed complete protection of SLAM- and nectin-4-blind virus-infected animals from viremia (Fig. 3E and F) and from clinical disease and death (Fig. 3G and H). In contrast, all contact animals experienced a typical course of disease associated with high cell-associated viremia (Fig. 3E and F) and 100% mortality (Fig. 3G and H), demonstrating formally that usage of both SLAM and nectin-4 receptors is essential for CDV transmission.

Biting may account for a nectin-4-blind virus transmission event. We observed two unexpected events in our SLAM- and nectin-4-blind transmission studies: one case of transmission of a nectin-4-blind CDV and a short-lived viremia in one animal infected with the SLAM-blind virus (Table 1). To assess whether CDV genomic mutations accounted for these events, we sequenced the H genes of the relevant viruses and found that the H gene from the transmitted nectin-4-blind virus was identical to that of the input virus carrying the P493S and Y539A mutations, which abolish entry through nectin-4 (Fig. 4A) (26). Since the infected animal did not develop signs of disease and frequent fighting was observed in this pair, direct contact between infected circulating immune cells and the oral mucosa of the contact animal during biting is a possible mode of transmission, in a manner similar to the natural transmission of feline immunodeficiency virus (FIV), where a blood-borne virus is transmitted by biting or other aggressive intraspecific behavior (41). Fighting between other animals, however, was infrequent, and no injuries were noted.

Compensatory mutations within or close to the SLAM-binding surface account for transient viremia. In contrast, sequence analysis of the H gene of the CDV causing transient viremia revealed three differences from the input virus. Two of the changes were either in the H protein surface interacting with SLAM (A529S) or immediately adjacent to it (S546Y) (Fig. 4B and C) (42). The third mutation (T192A) was located in a region of the stalk in close proximity to the globular head that stabilizes the β-sheet structure of the receptor-binding domain (Fig. 4B and C) (42). Presuming a partial reversion to a transmissible phenotype, we named this virus "SLAM-revertant" (SLAMrev).

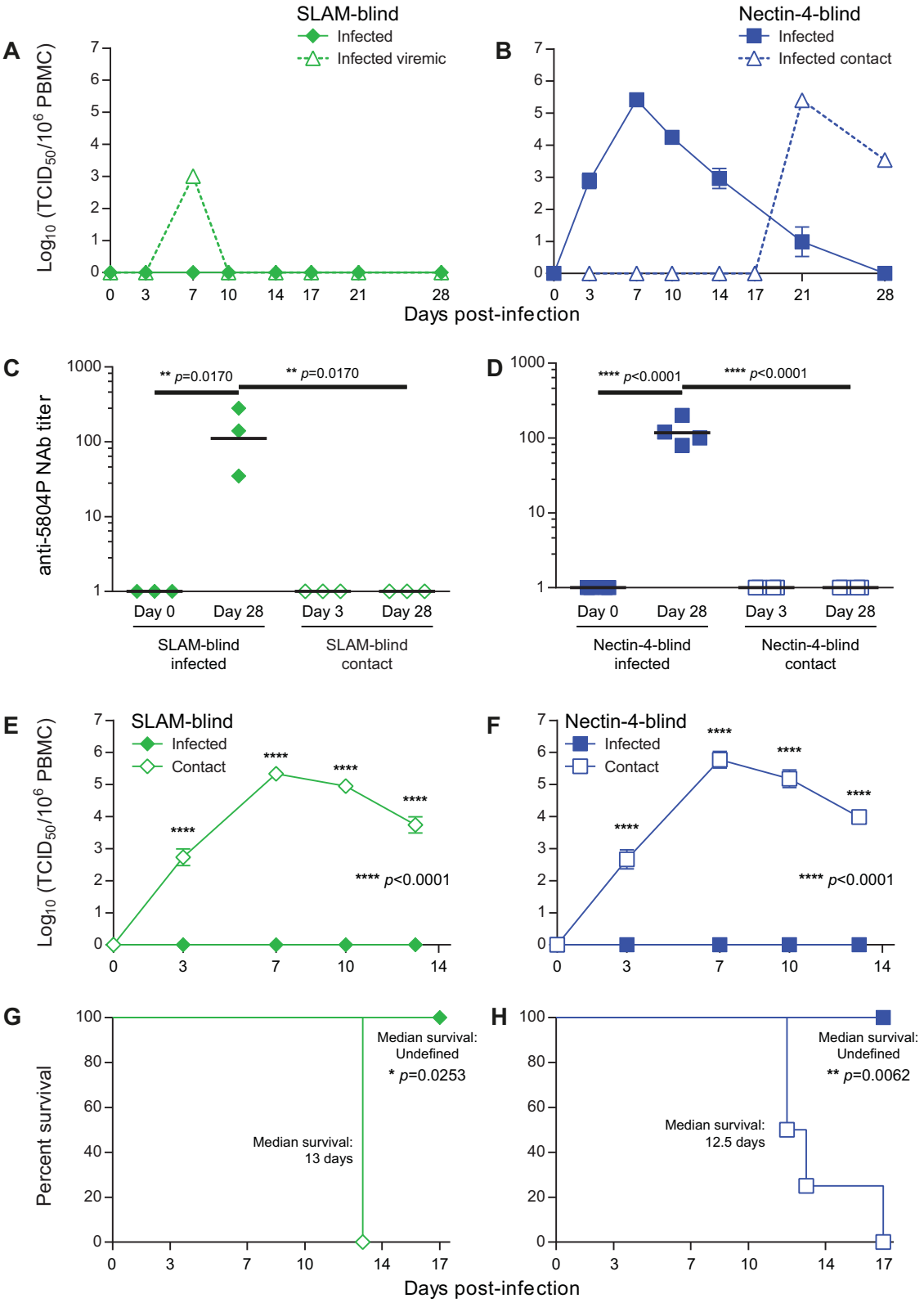

FIG 3 Lack of receptor-blind virus transmission. Relevant infected/contact pairs from the study shown in Table 1 were tested for antibodies against CDV and then challenged with the wild-type strain 5804PeH. (A and B) The course of cell-associated viremia is shown as the $\log_{10}$ of the virus titer per 10^6 PBMCs for animals infected with either the SLAM-blind ($n = 7$ infected/contact pairs) (A) or nectin-4-blind ($n = 8$ infected/contact pairs) (B) viruses. One SLAM-blind-infected animal that became viremic and one nectin-4-blind contact animal that became infected are shown separately as series with dashed lines in panels A and B, respectively. Days postinfection are indicated on the *x* axes, and error bars represent standard error of the mean. (C and D) CDV neutralizing responses

(Continued on next page)

TABLE 1 Transmission of SLAM- and nectin-4-blind CDVs

Condition	No. of animals with condition/total			
	SLAM-blind CDV		Nectin-4-blind CDV	
	Infected animals	Contact animals	Infected animals	Contact animals
Viremia	1/7	0/7	8/8	1/8
Immunosuppression[a]	0/7	0/7	8/8	1/8
Clinical signs[b]	0/7	0/7	0/8	0/8
Transmission	NA[c]	0/7	NA	1/8

[a]Immunosuppression was defined as having a decreased leukocyte count ($<1 \times 10^3$ PBMC/mm^3) and inhibition of PBMC proliferation after PHA stimulation (<20% of day 0 proliferation).
[b]Animals were monitored for fever, rash, and weight loss.
[c]NA, not applicable.

In addition to receptor binding, the H protein also provides fusion support, which is associated with conformational changes that in turn trigger fusion mediated by the F protein (43). We cloned the SLAMrev H into a eukaryotic expression plasmid and assessed the impact of the three mutations in the SLAMrev H protein on SLAM-mediated fusion support function. When coexpressed with the CDV F protein in VerodogSLAMtag cells, the H(SLAMrev) protein supported fusion at levels around 30 to 35% of those for the wild-type H protein (Fig. 4D). Introduction of the T192A and S546Y mutations into SLAM-blind H alone was sufficient to reach this level, whereas the A529S mutation had no effect and its combination with the spatially close S546Y mutation was also not beneficial (Fig. 4D).

To evaluate the impact of these changes on pathogenesis, a recombinant CDV was produced by exchanging the H gene of the wild-type virus 5804P with the H gene cDNA from the SLAMrev virus, which contains all three H mutations (Fig. 4E). We compared the biological characteristics of this virus with those of the wild-type and SLAM-blind isogenic strains by single- and multistep growth curve analysis. Wild-type CDV reached peak titers by 36 h after infection in the single-step growth curve, whereas the virus expressing H(SLAMrev) experienced a slight 12-h delay before reaching approximately the same titer, and the SLAM-blind virus did not replicate appreciably (Fig. 4F). In the multistep growth curve, wild-type and H(SLAMrev) viruses grew to similar peak titers, with the H(SLAMrev) virus again displaying a slight growth delay for the first 36 h, while the SLAM-blind virus replicated very poorly (Fig. 4G). The virus expressing the SLAMrev H protein is thus slightly impaired in its ability to enter immune cells but ultimately replicates with efficiency similar to that of the wild-type virus.

To assess its ability to infect and disseminate in immune cells *in vivo*, we infected two ferrets with the 5804PeH-H(SLAMrev) CDV and cohoused each animal with a naive contact starting 3 days after infection. Both infected animals developed viremia, which was cleared in the second week after infection, but the contacts remained uninfected (Fig. 5A). Both infected animals had transient moderate to high fever (39.5°C and 40.5°C) between days 5 and 10 after infection (Fig. 4B), and no other clinical signs were observed (data not shown). Only the infected animals

FIG 3 Legend (Continued)
in plasma. Antibody titers are shown as the reciprocal of the highest dilution at which CPE was observed. Data are shown for SLAM-blind-infected and contact animals (C) and nectin-4-blind-infected and contact animals (D). Plasma samples were tested from the day of infection (day 0) and after all animals had cleared the nectin-4-blind infection (day 28). The geometric mean neutralizing titer is indicated by a horizontal black bar for each group, and each symbol represents one animal. (E and F) Wild-type CDV challenge of SLAM-blind- and nectin-4-blind-infected and contact animals on day 35. Cell-associated viremia is shown as the $\log_{10}$ of the virus titer per 10^6 PBMCs for either SLAM-blind-infected animals (E) or nectin-4-blind-infected animals (F) and their respective contact animals. Days postinfection are indicated on the *x* axes, and error bars represent standard error of the mean. (G and H) Survival of SLAM-blind-infected and contact animals (G) or nectin-4-blind-infected and contact animals (H) after wild-type CDV challenge. The death of an animal is indicated by a step down on the curve, and median survival is indicated on each graph. Animals numbers are $n = 3$ infected/contacts pairs in panels C to H. Statistical significance in panels C to F was determined by one-way analysis of variance (ANOVA) and Fisher least-significant difference (LSD) posttest. The survival curves in panels G and H were compared by Mantel-Cox analysis.

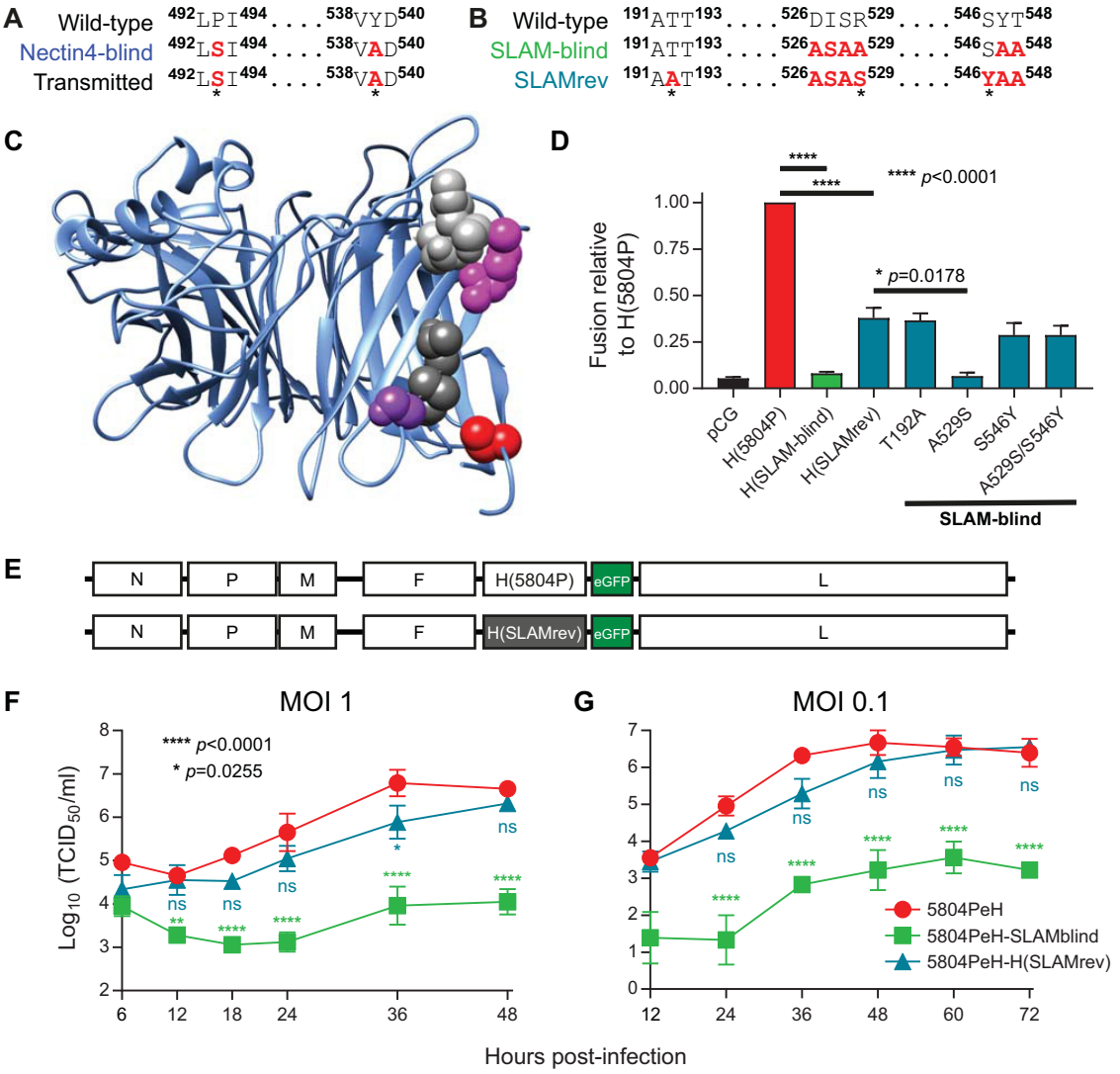

FIG 4 H protein sequence of a transmitted nectin-4-blind virus (A) and functional characterization of the H gene of the SLAMrev CDV (B to G). (A) Sequences of the nectin-4-binding residues of the H gene from the virus isolated from the contact animal (bottom) compared with those of the parental wild-type virus (top) and the input nectin-4-blind virus (center). (B) Amino acid sequences of the SLAM-binding domains of virus isolated from the viremic animal are shown in comparison to the corresponding regions in the parental wild-type virus and the input SLAM-blind virus used for this study. (C) Structural model of the CDV H protein globular head domain with location of the mutated residues. CDV H is shown as a ribbon structure, and the substitutions A529S and S546Y are shown as magenta and purple space-filling residues, respectively. The adjacent SLAM-binding residues at positions 526 to 528 and 547 to 548 are shown in light gray and dark gray, respectively. The T192A substitution is shown in red. (D) Assessment of recombinant H protein fusion support efficiency. VerodogSLAMtag cells transfected with plasmids expressing CDV F, the respective H genes, a RenLuc constitutive reporter, and ffLuc driven by the T7RNAP promoter were overlaid with VerodogSLAMtag cells transfected with a plasmid expressing T7RNAP under the control of the chicken β-actin promoter. The ffLuc signal from triplicate wells was normalized to the respective RenLuc control for each well. The normalized values were then expressed relative to the H(5804P) control for each replicate, which was set at 1. Error bars represent standard error of the mean. Statistical significance was determined by one-way ANOVA with Fisher LSD posttest. H(SLAM-blind) and H(SLAMrev) were compared to H(5804P), and H(SLAM-blind)-A529S was compared to H(SLAMrev). (E) Schematic of the genome of the parental 5804PeH and mutant 5804PeH-H(SLAMrev) recombinant genomes. (F and G) *In vitro* growth kinetics of the recombinant 5804PeH virus expressing the H(SLAMrev) protein in purified ferret PBMCs. Cells were infected with the respective viruses at an MOI of 1 (F) or 0.1 (G), and culture supernatants were harvested at the time points indicated on each graph. Titers are expressed as $TCID_{50}$/ml, and error bars indicate standard error of the mean. Statistical significance in panel F and G was determined by comparing the mutant viruses to wild-type 5804PeH at each time point by one-way ANOVA with Fisher LSD posttest.

developed neutralizing antibodies against wild-type CDV (Fig. 5C), again indicating that no subclinical transmission occurred. Thus, while enabling infection of lymphoid cells, the virus expressing the H(SLAMrev) was attenuated in ferrets and was not transmitted to naive hosts.

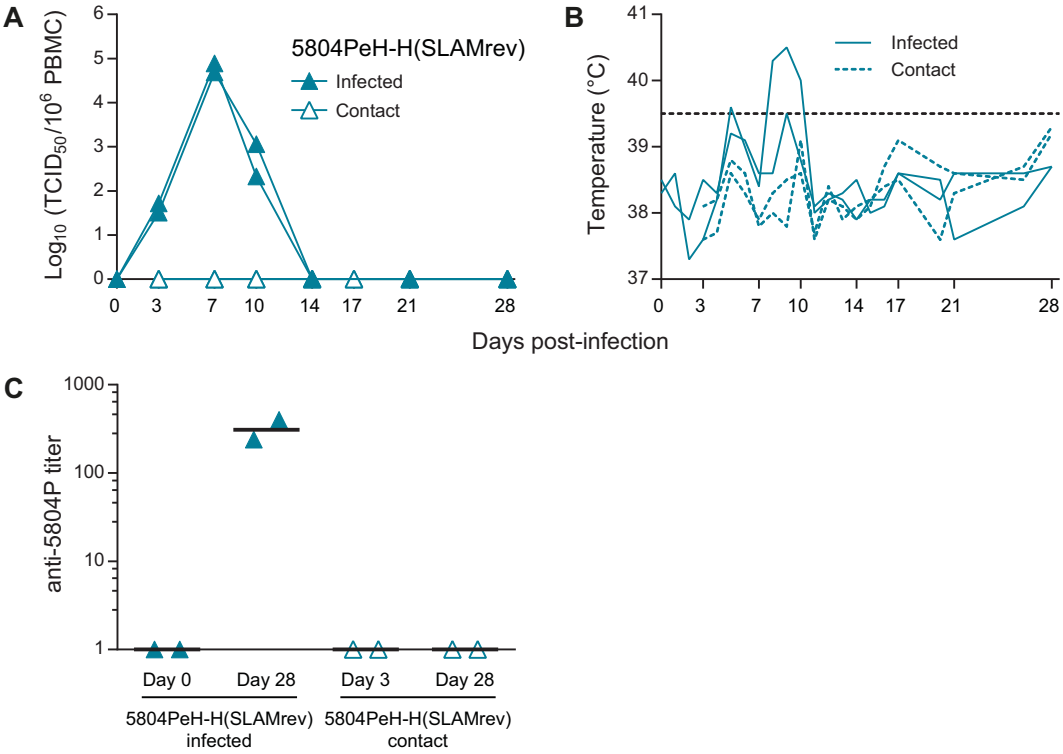

FIG 5 Pathogenesis of mutant 5804PeH-H(SLAMrev). Two ferrets were infected intranasally with 2×10^5 $TCID_{50}$ of 5804PeH-H(SLAMrev). Three days later, each animal was cohoused with a naive contact animal. (A) Course of cell-associated viremia shown as $\log_{10}$ of the virus titer per 10^6 PBMCs. (B) Temperatures of infected and contact animals. Each line in panels A and B represents one animal. Days postinfection are indicated on the *x* axes of the graphs. The dashed horizontal line at 39.5°C in panel B indicates the threshold for fever. (C) CDV neutralizing responses against 5804PeH-H(SLAMrev) in plasma. Antibody titers are shown as the reciprocal of the highest dilution at which CPE was observed for 5804PeH-H(SLAMrev)-infected and contact animals. Plasma samples were tested upon infection and after all animals had cleared infection (day 28). The geometric mean neutralizing titer is indicated by a horizontal black bar for each group; each symbol represents one animal.

DISCUSSION

Morbilliviruses are among the most transmissible viruses known, but their transmission determinants are poorly characterized. By comparing the timing and efficiency of transmission of wild-type and selectively receptor-blind CDVs in ferrets, we found that contact transmission of wild-type virus can precede the onset of clinical signs. Furthermore, our data formally prove that sequential interaction with both the SLAM and nectin-4 receptors is essential for transmission to naive hosts. Interestingly, three compensatory mutations were detected in a virus that was originally SLAM blind but caused mild viremia. However, expression of the corresponding H protein in the context of a wild-type genome was not sufficient to restore transmission.

SLAM-blind viruses replicate, but where? While it was known that infection of ferrets with the SLAM-blind virus used in this study (32), as well as infections of monkeys with a similar SLAM-blind MeV (28), induces strong adaptive immunity, the SLAMrev CDV described here is the first revertant identified in an infected animal. Indeed, accumulation of three mutations in the H gene suggests that the inoculated virus must have replicated. Even though we isolated SLAMrev from peripheral blood mononuclear cells (PBMCs), it seems likely that primary infection and replication occurred in other cell types, perhaps antigen-presenting cells such as dendritic cells (DCs).

DCs that express SLAM can be infected by morbilliviruses, but these viruses can also bind to DCs by interacting with the cell surface lectin DC-SIGN (44). Infected DCs then home to local draining lymph nodes, where infection is transmitted to SLAM-expressing lymphocytes (16, 45, 46). Since SLAM-blind viruses captured by DCs in the respiratory

tract would not be able to transfer to lymphocytes, an immune response similar to that observed with monkeys vaccinated intramuscularly with MeV (17) is the most likely explanation for the sterilizing immunity that we observed here. It cannot be excluded, however, that limited replication in epithelial cells occurs, since the nectin-4-binding site of SLAM-blind CDV remains intact (27). Localized infection of epithelial cells in the respiratory tract could recruit antigen-presenting cells to respond to the infection, and this may also contribute to the strong immunity induced by SLAM-blind viruses.

Efficient transmission requires virus release from the respiratory epithelium. CDV transmission has been demonstrated using both contact and aerosol models (7, 29, 47), and animals with obvious signs of clinical disease easily transmit the virus to naive hosts in both setups. The distribution of viral receptors is likely a key determinant in efficient transmission. Infection of epithelial cells is initiated when CDV-infected PBMCs contact the basolateral surface of the respiratory epithelium, where nectin-4 is expressed as part of the apical junction complex (18, 20–22). Virus is then released from the apical surface of infected respiratory epithelial cells into the lumen, where neither nectin-4 nor SLAM is expressed. The release of newly produced virus particles would therefore not be hindered by receptor binding interactions, facilitating spread as respiratory droplets or by aerosol. Indeed, we detected cell-free MeV in the respiratory tract of monkeys (22) and in the urinary tract of ferrets (26), further supporting this idea. Even if occasional CDV transmission by biting can occur, our studies demonstrate that morbillivirus infection of epithelial cells is a prerequisite for efficient transmission.

Compensatory mutations highlight selective pressure on SLAM-dependent cell entry. The spatial vicinity of all three mutations to the SLAM footprint on the H protein (48) detected here is consistent with an essential role of SLAM binding for morbillivirus spread in natural hosts, but are the substitutions documented here also observed in natural CDV isolates?

Some South African isolates have an M195I substitution (49) located close to the T192A mutation in our SLAMrev virus. A different substitution at this position (M195V) may influence receptor binding (39). Many isolates of the Asia-I lineage have a Y549H substitution (50), which is immediately adjacent to residues 547/548 mutated in the SLAM-blind virus. This substitution also occurs frequently in combination with an I542N mutation, which introduces a potential N-linked glycosylation site (50). Several Asia-II lineage isolates from South Korea have a T548M substitution (51), which alters one of the residues in the second SLAM-binding cluster, and a South Korean isolate has a D526G substitution in the first SLAM-binding cluster (https://www.ncbi.nlm.nih.gov/nuccore/eu252148). A S546F substitution in another South Korean isolate (52) coincides with the S546Y mutation in SLAMrev. Even if the functional consequences of these mutations have not been investigated, the presence of substitutions in similar H protein locations suggests that circulating CDV isolates are subject to the same SLAM-dependent cell entry selective pressure documented here.

Our work demonstrates the importance of sequential use of the SLAM and nectin-4 receptors in CDV pathogenesis and transmission. Strong *in vivo* selective pressure drives the H gene toward efficient interaction with SLAM, selecting compensating mutations in or near the SLAM-interacting surface. However, suboptimal SLAM interactions lead to inefficient lymphocyte infection, which interrupts the transmission cycle. Since morbillivirus glycoproteins have limited inherent capacity for antigenic variation (48, 53), strategies to reduce H protein-SLAM interactions, disrupting transmission, may be useful for generating new vaccines.

MATERIALS AND METHODS

Cells and viruses. Vero cells stably expressing the canine SLAM receptor (VerodogSLAMtag) (30) were maintained in Dulbecco's modified Eagle medium (DMEM) (Sigma) containing 5% heat-inactivated fetal bovine serum (FBS) (Gibco). The recombinant parental 5804PeH expresses enhanced green fluorescent protein (eGFP) from an additional gene inserted between the hemagglutinin (H) and polymerase (L) genes (31). The recombinant SLAM-blind (32) and nectin-4-blind (26) mutant viruses use the 5804PeH genomic backbone and have been reported in prior publications. All viruses were grown on VerodogSLAMtag cells, and titrations were performed by limiting dilution and expressed as 50% tissue culture infectious doses ($TCID_{50}$).

Transmission studies. Unvaccinated male and female ferrets (*Mustela putoris furo*) 16 weeks or older were housed in the Paul-Ehrlich-Institut animal facility. All animal studies were approved by the Institutional Animal Care Committee according to German and European regulations. For initial studies with 5804PeH and all studies with SLAM- and nectin-4-blind viruses, groups of three or four animals were infected intranasally with 2×10^5 $TCID_{50}$ of the respective viruses and housed individually for 3 days. At 3 days postinfection, the infected animals were cohoused with a naive contact animal for the remainder of the experiment. The infected/contact pairs were monitored daily for clinical signs of fever, rash, activity, depression, and weight loss. For day-of-transmission studies, contact animals were cohoused with infected animals for 24 h on days 4 and 5, 5 and 6, and 6 and 7 or for 48 h on days 6 and 7, 8 and 9, and 10 and 11 after initial infection and then were moved to separate cages. Blood samples were collected twice weekly from the superior vena cava under general anesthesia for the first 3 weeks and weekly thereafter. Cell-associated viremia in peripheral blood mononuclear cells (PBMCs) was quantified by limiting dilution (32) and expressed as $TCID_{50}/10^6$ PBMCs. The extent of PBMC proliferation inhibition was measured by stimulation of Histopaque-purified PBMCs with 2 μg/ml of phytohemagglutin M (PHA) and subsequent detection of bromodeoxyuridine (BrdU) incorporation into proliferating cells using a cell proliferation BrdU enzyme-linked immunosorbent assay (ELISA) kit (Roche). Since the SLAM- and nectin-4-blind viruses are completely attenuated and all animals survived infection, one group of 3 infected/contact pairs from each virus was subsequently challenged intranasally with 2×10^5 $TCID_{50}$ of 5804PeH to confirm that infected animals had indeed developed immunity while contact animals had in fact not been infected and were thus still susceptible to lethal disease.

VNTs. For virus neutralization tests (VNTs), neutralizing-antibody titers were determined by mixing serial dilutions of plasma collected before infection (day 0) or contact (day 3) and at the end of the study (day 28) with 10^2 $TCID_{50}$ of 5804PeH. The virus and plasma dilutions were incubated at 37°C for 15 min before 50 μl of VerodogSLAMtag cells was added to each well. The neutralizing titer was expressed as the reciprocal of the highest dilution at which no cytopathic effect (CPE) was observed after 3 days.

Mutant H gene cloning and mutagenesis. Viral RNA was isolated using the RNeasy minikit (Qiagen) from VerodogSLAMtag cells infected with the SLAM-revertant (SLAMrev) virus, which was originally obtained from one animal that had transient viremia on day 7 after infection with SLAM-blind CDV. The RNA was reverse transcribed with SuperScript III reverse transcriptase (Invitrogen) according to the manufacturer's recommendations.

The H gene and flanking regions were amplified from the resulting cDNA using primers that bind in the F gene transmembrane domain and the 5′ terminus of the eGFP gene and then were sequenced. The expression plasmid pCG-CDV H(SLAMrev) was generated by amplifying the SLAMrev H open reading frame (ORF) and cloning into the BamHI and SphI sites of pCG-IRESzeomut (30). The mutations T192A, A529S, and S546Y found in the SLAMrev H gene were introduced individually and in combination into the SLAM-blind H gene expression plasmid by site-directed mutagenesis using *Pfu* DNA polymerase.

To generate the genomic plasmid p5804PeH-H(SLAMrev), the H ORF of the SLAMrev virus was amplified and joined to the subgenomic cassette between the BsrGI and AscI sites by overlapping PCR. This construct was then transferred into the full-length p5804PeH plasmid, which expresses the enhanced green fluorescent protein (eGFP) from an additional open reading frame located between the H and L genes (31). All plasmids were verified by sequencing, as were all viruses after successful recovery.

Recovery of recombinant viruses and growth kinetics. A recombinant virus expressing the SLAMrev H protein was recovered as described previously (26, 54), with modifications. Briefly, 293 cells were seeded into six-well dishes at a density of 7×10^5 cells per well. The next day, cells were transfected with 8 μg of p5804PeH-H(SLAMrev) and combinations of 0.5, 0.1, 0.5, and 0.7 μg MeV N, P, and polymerase (L) and T7 RNA polymerase (RNAP) expression plasmids, respectively, using 12.5 μl TurboFect (Thermo Fisher) per well. Three to five days later, the transfected cells were transferred onto VerodogSLAMtag cells seeded at 80 to 90% confluence in 10-cm dishes. Individual syncytia were inoculated onto fresh VerodogSLAMtag cells. Stocks of all viruses used in this study were produced on VerodogSLAMtag cells. Titers were determined by limiting dilution and expressed as 50% tissue culture infectious doses ($TCID_{50}$).

***In vitro* growth kinetics in ferret PBMCs.** PBMCs were isolated from heparinized whole ferret blood by Histopaque-1077 centrifugation for 40 min at 400 $\times$ *g*. The cells were washed three times with phosphate-buffered saline (PBS) and then resuspended in RPMI 1640 medium (BioWest) containing 10% FBS and 1% L-glutamine. For single- and multistep growth curves, purified PBMCs were seeded in round-bottom 96-well plates at a density of 2.5×10^5 cells/well and were stimulated overnight with 5 μg/ml concanavalin A (ConA) (Sigma). The following day, cells from the respective animals were resuspended, pooled, and washed with PBS. Cells were then infected with the respective viruses at a multiplicity of infection (MOI) of either 1 or 0.1 for 1 h. Unadsorbed virus was removed by washing three times with PBS. PBMCs were incubated in round-bottom 96-well plates in RPMI containing 5 μg/ml ConA at 37°C. Culture supernatants were harvested daily by transfer of the cell suspension into fresh Eppendorf tubes. PBMCs were pelleted by centrifugation at 1,000 $\times$ *g* for 5 min. The supernatants were transferred to fresh Eppendorf tubes and stored at −80°C, and virus in the supernatant fractions was determined by $TCID_{50}$ assay.

Quantitative fusion assays. Quantitative fusion assays were performed as previously described (55), with modifications. Confluent monolayers of VerodogSLAMtag cells in a 6-well dish were transfected with 5 μg/well of pCAGGS-T7RNAP, which expresses the bacteriophage T7 DNA-dependent RNA polymerase (T7RNAP) under the control of the chicken β-actin promoter. The transfected cells were trypsinized 18 h later and pooled for use as target cells in the assay. In parallel, 10^5 VerodogSLAMtag cells were seeded into black flat-bottom 96-well dishes. These cells were transfected with 0.25 μg/well of plasmid containing the firefly luciferase (ffLuc) gene under the control of the T7RNAP promoter (pTM1-ffLuc) along with 0.125 μg/well of expression plasmid for the CDV F protein and 0.125 μg/well of expression

plasmid for the respective CDV H proteins, as well as 0.25 μg/well of a control plasmid expressing *Renilla* luciferase (RenLuc) under the control of the thymidine kinase promoter (pRL-TK) (Promega). After incubation for 6 h at 37°C, 10^4 T7RNAP-expressing target cells/well were added to the 96-well dishes and were incubated at 37°C for 24 h. Assays were developed using the Dual-Glo luciferase assay system (Promega). Cells were lysed with 75 μl/well of Dual-Glo reagent and incubated at room temperature for 10 min. The firefly luciferase was then read in a PheraStar luminometer. Next, 75 μl/well Dual-Glo Stop & Glo reagent was added to each well and incubated at room temperature for 10 mins, and the *Renilla* luciferase signal was read. The firefly luciferase signal was divided by the *Renilla* luciferase signal for each respective well to generate the normalized luciferase signal. Values from each triplicate transfection were averaged and are expressed as the fusion relative to wild type H(5804P) for each experiment. Fusion studies were performed three times.

CDV H protein structural modeling. The H protein sequence of the 5804P strain (AY386316) was queried in the Phyre2 Protein Fold Recognition Server database (56), and a structural model was generated using the crystal structure of MeV H in complex with human SLAM (PDB 3ALW) as a template (48). The resulting PDB file was annotated using UCSF Chimera version 1.12 (57).

ACKNOWLEDGMENTS

We thank Yvonne Krebs for technical assistance and help with animal experiments, and we thank all von Messling and Cattaneo laboratory members for thoughtful and stimulating discussions.

This work was funded by the German Bundesministerium für Gesundheit, the German Center for Infection Research (DZIF), and German Research Foundation Collaborative Research Center SFB 1021 (V.V.M.).

REFERENCES

1. Ludlow M, Rennick LJ, Nambulli S, de Swart RL, Duprex WP. 2014. Using the ferret model to study morbillivirus entry, spread, transmission and cross-species infection. Curr Opin Virol 4:15–23. https://doi.org/10.1016/j.coviro.2013.11.001.
2. Guerra FM, Bolotin S, Lim G, Heffernan J, Deeks SL, Li Y, Crowcroft NS. 2017. The basic reproduction number (R_0) of measles: a systematic review. Lancet Infect Dis 17:e420–e428. https://doi.org/10.1016/S1473-3099(17)30307-9.
3. de Swart RL, Duprex WP, Osterhaus ADME. 2012. Rinderpest eradication: lessons for measles eradication? Curr Opin Virol 2:330–334. https://doi.org/10.1016/j.coviro.2012.02.010.
4. Anderson RM, May RM. 1982. Directly transmitted infectious diseases: control by vaccination. Science 215:1053–1060. https://doi.org/10.1126/science.7063839.
5. Fraser C, Donnelly CA, Cauchemez S, Hanage WP, Van Kerkhove MD, Hollingsworth TD, Griffin J, Baggaley RF, Jenkins HE, Lyons EJ, Jombart T, Hinsley WR, Grassly NC, Balloux F, Ghani AC, Ferguson NM, Rambaut A, Pybus OG, Lopez-Gatell H, Alpuche-Aranda CM, Chapela IB, Zavala EP, Guevara DME, Checchi F, Garcia E, Hugonnet S, Roth C, The WHO Rapid Pandemic Assessment Collaboration. 2009. Pandemic potential of a strain of influenza A (H1N1): early findings. Science 324:1557–1561. https://doi.org/10.1126/science.1176062.
6. Griffin DE. 2015. Measles virus, p 1042–1069. *In* Knipe DM, Howley PM (ed), Fields virology, 6th ed, vol 1. Lippincott Williams & Wilkins, Philadelphia, PA.
7. de Vries RD, Ludlow M, de Jong A, Rennick LJ, Verburgh RJ, van Amerongen G, van Riel D, van Run PRWA, Herfst S, Kuiken T, Fouchier RAM, Osterhaus ADME, de Swart RL, Duprex WP. 2017. Delineating morbillivirus entry, dissemination and airborne transmission by studying in vivo competition of multicolor canine distemper viruses in ferrets. PLoS Pathog 13:e1006371. https://doi.org/10.1371/journal.ppat.1006371.
8. Bischoff WE, McNall RJ, Blevins MW, Turner J, Lopareva EN, Rota PA, Stehle JJR. 2016. Detection of measles virus RNA in air and surface specimens in a hospital setting. J Infect Dis 213:600–603. https://doi.org/10.1093/infdis/jiv465.
9. Varble A, Albrecht RA, Backes S, Crumiller M, Bouvier NM, Sachs D, García-Sastre A, ten Oever BR. 2014. Influenza A virus transmission bottlenecks are defined by infection route and recipient host. Cell Host Microbe 16:691–700. https://doi.org/10.1016/j.chom.2014.09.020.
10. Frise R, Bradley K, van Doremalen N, Galiano M, Elderfield RA, Stilwell P, Ashcroft JW, Fernandez-Alonso M, Miah S, Lackenby A, Roberts KL, Donnelly CA, Barclay WS. 2016. Contact transmission of influenza virus between ferrets imposes a looser bottleneck than respiratory droplet transmission allowing propagation of antiviral resistance. Sci Rep 6:29793. https://doi.org/10.1038/srep29793.
11. Hope K, Boyd R, Conaty S, Maywood P. 2012. Measles transmission in health care waiting rooms: implications for public health response. Western Pac Surveill Response J 3:33–38. https://doi.org/10.5365/wpsar.2012.3.3.009.
12. Tatsuo H, Ono N, Tanaka K, Yanagi Y. 2000. SLAM (CDw150) is a cellular receptor for measles virus. Nature 406:893–897. https://doi.org/10.1038/35022579.
13. Tatsuo H, Ono N, Yanagi Y. 2001. Morbilliviruses use signaling lymphocyte activation molecules (CD150) as cellular receptors. J Virol 75:5842–5850. https://doi.org/10.1128/JVI.75.13.5842-5850.2001.
14. Baron MD. 2005. Wild-type *Rinderpest virus* uses SLAM (CD150) as its receptor. J Gen Virol 86:1753–1757. https://doi.org/10.1099/vir.0.80836-0.
15. Koethe S, Avota E, Schneider-Schaulies S. 2012. Measles virus transmission from dendritic cell to T cells: formation of synapse-like interfaces concentrating viral and cellular components. J Virol 86:9773–9781. https://doi.org/10.1128/JVI.00458-12.
16. Mesman AW, de Vries RD, McQuaid S, Duprex WP, de Swart RL, Geijtenbeek TBH. 2012. A prominent role for DC-SIGN$^+$ dendritic cells in initiation and dissemination of measles virus infection in non-human primates. PLoS One 7:e49573. https://doi.org/10.1371/journal.pone.0049573.
17. Rennick LJ, de Vries RD, Carsillo TJ, Lemon K, van Amerongen G, Ludlow M, Nguyen DT, Yüksel S, Verburgh RJ, Haddock P, McQuaid S, Duprex WP, de Swart RL. 2015. Live-attenuated measles virus vaccine targets dendritic cells and macrophages in the muscle of nonhuman primates. J Virol 89:2192–2200. https://doi.org/10.1128/JVI.02924-14.
18. Mühlebach MD, Mateo M, Sinn PL, Prüfer S, Uhlig KM, Leonard VHJ, Navaratnarajah CK, Frenzke M, Wong XX, Sawatsky B, Ramachandran S, McCray PB, Cichutek K, von Messling V, Lopez M, Cattaneo R. 2011. Adherens junction protein nectin-4 is the epithelial receptor for measles virus. Nature 480:530–533. https://doi.org/10.1038/nature10639.
19. Noyce RS, Bondre DG, Ha MN, Lin L-T, Sisson G, Tsao M-S, Richardson CD. 2011. Tumor cell marker PVRL4 (nectin 4) is an epithelial cell receptor for measles virus. PLoS Pathog 7:e1002240. https://doi.org/10.1371/journal.ppat.1002240.
20. Ludlow M, Lemon K, de Vries RD, McQuaid S, Millar EL, van Amerongen G, Yüksel S, Verburgh RJ, Osterhaus ADME, de Swart RL, Duprex WP. 2013. Measles virus infection of epithelial cells in the macaque upper respiratory tract is mediated by subepithelial immune cells. J Virol 87:4033–4042. https://doi.org/10.1128/JVI.03258-12.
21. Ludlow M, de Vries RD, Lemon K, McQuaid S, Millar E, van Amerongen G,

Yüksel S, Verburgh RJ, Osterhaus ADME, de Swart RL, Duprex WP. 2013. Infection of lymphoid tissues in the macaque upper respiratory tract contributes to the emergence of transmissible measles virus. J Gen Virol 94:1933–1944. https://doi.org/10.1099/vir.0.054650-0.
22. Frenzke M, Sawatsky B, Wong XX, Delpeut S, Mateo M, Cattaneo R, von Messling V. 2013. Nectin-4-dependent measles virus spread to the cynomolgus monkey tracheal epithelium: role of infected immune cells infiltrating the lamina propria. J Virol 87:2526–2534. https://doi.org/10.1128/JVI.03037-12.
23. Singh BK, Hornick AL, Krishnamurthy S, Locke AC, Mendoza CA, Mateo M, Miller-Hunt CL, Cattaneo R, Sinn PL. 2015. The nectin-4/afadin protein complex and intercellular membrane pores contribute to rapid spread of measles virus in primary human airway epithelia. J Virol 89:7089–7096. https://doi.org/10.1128/JVI.00821-15.
24. Singh BK, Li N, Mark AC, Mateo M, Cattaneo R, Sinn PL. 2016. Cell-to-cell contact and nectin-4 govern spread of measles virus from primary human myeloid cells to primary human airway epithelial cells. J Virol 90:6808–6817. https://doi.org/10.1128/JVI.00266-16.
25. Leonard VHJ, Sinn PL, Hodge G, Miest T, Devaux P, Oezguen N, Braun W, McCray PB, Jr, McChesney MB, Cattaneo R. 2008. Measles virus blind to its epithelial cell receptor remains virulent in rhesus monkeys but cannot cross the airway epithelium and is not shed. J Clin Invest 118:2448–2458. https://doi.org/10.1172/JCI35454.
26. Sawatsky B, Wong X-X, Hinkelmann S, Cattaneo R, von Messling V. 2012. Canine distemper virus epithelial cell infection is required for clinical disease but not for immunosuppression. J Virol 86:3658–3666. https://doi.org/10.1128/JVI.06414-11.
27. von Messling V, Oezguen N, Zheng Q, Vongpunsawad S, Braun W, Cattaneo R. 2005. Nearby clusters of hemagglutinin residues sustain SLAM-dependent canine distemper virus entry in peripheral blood mononuclear cells. J Virol 79:5857–5862. https://doi.org/10.1128/JVI.79.9.5857-5862.2005.
28. Leonard VHJ, Hodge G, Reyes-del Valle J, McChesney MB, Cattaneo R. 2010. Measles virus selectively blind to signaling lymphocytic activation molecule (SLAM; CD150) is attenuated and induces strong adaptive immune responses in rhesus monkeys. J Virol 84:3413–3420. https://doi.org/10.1128/JVI.02304-09.
29. Shen DT, Gorham JR. 1978. Contact transmission of distemper virus in ferrets. Res Vet Sci 24:118–119.
30. von Messling V, Springfeld C, Devaux P, Cattaneo R. 2003. A ferret model of canine distemper virus virulence and immunosuppression. J Virol 77:12579–12591. https://doi.org/10.1128/JVI.77.23.12579-12591.2003.
31. von Messling V, Milosevic D, Cattaneo R. 2004. Tropism illuminated: lymphocyte-based pathways blazed by lethal morbillivirus through the host immune system. Proc Natl Acad Sci U S A 101:14216–14221. https://doi.org/10.1073/pnas.0403597101.
32. von Messling V, Svitek N, Cattaneo R. 2006. Receptor (SLAM [CD150]) recognition and the V protein sustain swift lymphocyte-based invasion of mucosal tissue and lymphatic organs by a morbillivirus. J Virol 80:6084–6092. https://doi.org/10.1128/JVI.00357-06.
33. Pillet S, von Messling V. 2009. Canine distemper virus selectively inhibits apoptosis progression in infected immune cells. J Virol 83:6279–6287. https://doi.org/10.1128/JVI.00050-09.
34. Moss WJ, Griffin DE. 2012. Measles. Lancet 379:153–164. https://doi.org/10.1016/S0140-6736(10)62352-5.
35. American Academy of Pediatrics. 2012. Measles, p 489–499. *In* Pickering LK, Baker CJ, Kimberlin DW, Long SS (ed), Red book: 2012 report of the Committee on Infectious Diseases, 29th ed. American Academy of Pediatrics, Elk Grove Village, IL.
36. Centers for Disease Control and Prevention. 2015. Measles virus, p 209–229. *In* Hamborsky J, Kroger A, Wolfe S (ed), Epidemiology and prevention of vaccine-preventable diseases (pink book), 13th ed. Public Health Foundation, Washington, DC.
37. Laksono B, de Vries R, McQuaid S, Duprex W, de Swart R. 2016. Measles virus host invasion and pathogenesis. Viruses 8:210. https://doi.org/10.3390/v8080210.
38. Mateo M, Navaratnarajah CK, Cattaneo R. 2014. Structural basis of efficient contagion: measles variations on a theme by parainfluenza viruses. Curr Opin Virol 5:16–23. https://doi.org/10.1016/j.coviro.2014.01.004.
39. Sattler U, Khosravi M, Avila M, Pilo P, Langedijk JP, Ader-Ebert N, Alves LA, Plattet P, Origgi FC. 2014. Identification of amino acid substitutions with compensational effects in the attachment protein of canine distemper virus. J Virol 88:8057–8064. https://doi.org/10.1128/JVI.00454-14.
40. Krakowka S, Cockerell G, Koestner A. 1975. Effects of canine distemper virus infection on lymphoid function in vitro and in vivo. Infect Immun 11:1069–1078.
41. Miller C, Boegler K, Carver S, MacMillan M, Bielefeldt-Ohmann H, Vande-Woude S. 2017. Pathogenesis of oral FIV infection. PLoS One 12:e0185138. https://doi.org/10.1371/journal.pone.0185138.
42. Navaratnarajah CK, Vongpunsawad S, Oezguen N, Stehle T, Braun W, Hashiguchi T, Maenaka K, Yanagi Y, Cattaneo R. 2008. Dynamic interaction of the measles virus hemagglutinin with its receptor signaling lymphocytic activation molecule (SLAM, CD150). J Biol Chem 283:11763–11771. https://doi.org/10.1074/jbc.M800896200.
43. Ader N, Brindley MA, Avila M, Origgi FC, Langedijk JPM, Örvell C, Vandevelde M, Zurbriggen A, Plemper RK, Plattet P. 2012. Structural rearrangements of the central region of the morbillivirus attachment protein stalk domain trigger F protein refolding for membrane fusion. J Biol Chem 287:16324–16334. https://doi.org/10.1074/jbc.M112.342493.
44. de Witte L, Abt M, Schneider-Schaulies S, van Kooyk Y, Geijtenbeek TBH. 2006. Measles virus targets DC-SIGN to enhance dendritic cell infection. J Virol 80:3477–3486. https://doi.org/10.1128/JVI.80.7.3477-3486.2006.
45. Lemon K, de Vries RD, Mesman AW, McQuaid S, van Amerongen G, Yüksel S, Ludlow M, Rennick LJ, Kuiken T, Rima BK, Geijtenbeek TBH, Osterhaus ADME, Duprex WP, de Swart RL. 2011. Early target cells of measles virus after aerosol infection of non-human primates. PLoS Pathog 7:e1001263. https://doi.org/10.1371/journal.ppat.1001263.
46. de Witte L, de Vries RD, van der Vlist M, Yüksel S, Litjens M, de Swart RL, Geijtenbeek TBH. 2008. DC-SIGN and CD150 have distinct roles in transmission of measles virus from dendritic cells to T-lymphocytes. PLoS Pathog 4:e1000049. https://doi.org/10.1371/journal.ppat.1000049.
47. Gorham JR, Brandly CA. 1953. The transmission of distemper among ferrets and mink, p 129–141. *In* Proceedings of the 90th Annual American Veterinary Medical Association Meeting. American Veterinary Medical Association, Toronto, Ontario, Canada.
48. Hashiguchi T, Ose T, Kubota M, Maita N, Kamishikiryo J, Maenaka K, Yanagi Y. 2011. Structure of the measles virus hemagglutinin bound to its cellular receptor SLAM. Nat Struct Mol Biol 18:135–141. https://doi.org/10.1038/nsmb.1969.
49. Woma TY, van Vuuren M, Bosman A-M, Quan M, Oosthuizen M. 2010. Phylogenetic analysis of the haemagglutinin gene of current wild-type canine distemper viruses from South Africa: lineage Africa. Vet Microbiol 143:126–132. https://doi.org/10.1016/j.vetmic.2009.11.013.
50. Zhao J, Zhang H, Bai X, Martella V, Hu B, Sun Y, Zhu C, Zhang L, Liu H, Xu S, Shao X, Wu W, Yan X. 2014. Emergence of canine distemper virus strains with two amino acid substitutions in the haemagglutinin protein, detected from vaccinated carnivores in North-Eastern China in 2012-2013. Vet J 200:191–194. https://doi.org/10.1016/j.tvjl.2014.01.028.
51. An D-J, Yoon S-H, Park J-Y, No I-S, Park B-K. 2008. Phylogenetic characterization of canine distemper virus isolates from naturally infected dogs and a marten in Korea. Vet Microbiol 132:389–395. https://doi.org/10.1016/j.vetmic.2008.05.025.
52. Lan NT, Yamaguchi R, Hirai T, Kai K, Morishita K. 2009. Relationship between growth behavior in Vero cells and the molecular characteristics of recent isolates classified in the Asia 1 and 2 groups of canine distemper virus. J Vet Med Sci 71:457–461. https://doi.org/10.1292/jvms.71.457.
53. Fulton BO, Sachs D, Beaty SM, Won ST, Lee B, Palese P, Heaton NS. 2015. Mutational analysis of measles virus suggests constraints on antigenic variation of the glycoproteins. Cell Rep 11:1331–1338. https://doi.org/10.1016/j.celrep.2015.04.054.
54. Martin A, Staeheli P, Schneider U. 2006. RNA polymerase II-controlled expression of antigenomic RNA enhances the rescue efficacies of two different members of the *Mononegavirales* independently of the site of viral genome replication. J Virol 80:5708–5715. https://doi.org/10.1128/JVI.02389-05.
55. Sawatsky B, Bente DA, Czub M, von Messling V. 2016. Morbillivirus and henipavirus attachment protein cytoplasmic domains differently affect protein expression, fusion support, and particle assembly. J Gen Virol 97:1066–1076. https://doi.org/10.1099/jgv.0.000415.
56. Kelley LA, Mezulis S, Yates CM, Wass MN, Sternberg MJE. 2015. The Phyre2 web portal for protein modeling, prediction and analysis. Nat Protoc 10:845–858. https://doi.org/10.1038/nprot.2015.053.
57. Pettersen EF, Goddard TD, Huang CC, Couch GS, Greenblatt DM, Meng EC, Ferrin TE. 2004. UCSF Chimera—a visualization system for exploratory research and analysis. J Comput Chem 25:1605–1612. https://doi.org/10.1002/jcc.20084.